PHYSICAL REVIEW B VOLUME 50, NUMBER 15 15 OCTOBER 1994-I

Skutterudite antimonides: Quasilinear bands and unusual transport

David J. Singh and Warren E. Pickett
Complex Systems Theory Branch, Naval Research Laboratory, Washington, D.C. 20375
(Received 29 July 1994; revised manuscript received 24 August 1994)

Electronic-structure calculations are reported for $IrSb_3$, $CoSb_3$, and $CoAs_3$ in the skutterudite structure. The band structures show a pseudogap around the Fermi level. The single band, which crosses the pseudogap, touches the conduction-band minimum at the Γ point in $CoAs_3$ and $IrSb_3$ and almost touches it in $CoSb_3$ due to a different ordering of the conduction bands. The dispersion of this gap-crossing band is quadratic at the Γ point as expected, but for the antimonides it remarkably crosses over to linear behavior extremely close to the band edge, so that for doping levels as low as 3×10^{16} holes/cm^3 the properties are determined by the linear dispersion. This yields interesting transport effects, such as a completely off-diagonal inverse mass tensor and unusual doping dependencies of the hole mobility and Seebeck coefficient. The Seebeck coefficients calculated from the band dispersion are in excellent agreement with experiment.

Skutterudite pnictides, MA_3, where M is Co, Rh, or Ir and A is P, As, or Sb, have been considered likely candidates for advanced thermoelectric (TE) materials.[1,2] For use in the construction of efficient TE systems, a material should have a high electrical conductivity, a low thermal conductivity, and a high Seebeck coefficient. As synthesized, unoptimized $IrSb_3$ samples reported by Slack and Tsoukala[2] (ST) have reasonably large Seebeck coefficients of approximately $S=72$ μV/K combined with very high hole mobilities and low thermal conductivities κ. ST have speculated, based on the minimum thermal-conductivity model,[3] that κ may be reduced by as much as a factor of 40 without strongly affecting the electrical conductivity σ, by structural modifications such as insertion of heavy electronically neutral atoms into the large voids that exist in the crystal structure to form the filled skutterudite structure or by alloying. Expected dependencies of σ and S suggest that optimization of the doping levels may improve these values. TE performance exceeding that of any known material would be obtained if the figure of merit $Z=\sigma S^2/\kappa$ could be increased by a factor of 5 over that of these unoptimized samples. Another possibility is that enhanced properties may be discovered in one of the related skutterudites; the other antimonides seem most likely, since their thermal conductivities may not be degraded relative to $IrSb_3$.[4]

The skutterudites occur in a bcc $Im3$ structure with four formula units per cell and may be regarded as formed from the cubic perovskite structure $\square MA_3$ ($\square$ denotes an empty site) with tilts of the octahedra such that the anions move along the cube faces to form nearly square four-membered rings. Relatively little is known about the electronic structures of these compounds except that they are doped insulators and seem to have substantial band gaps, e.g., 1.4 eV measured spectroscopically in $IrSb_3$,[2] although Ackermann and Wold report finding no optical gap in $CoAs_3$ and $CoSb_3$.[5] No self-consistent band-structure calculations have been reported, perhaps because of the complex crystal structure that results in a relatively open unit cell containing 16 atoms.[6]

In order to understand the properties from a microscopic point of view we have performed local-density approximation electronic-structure calculations for $IrSb_3$, as well as for the related skutterudites $CoSb_3$ and $CoAs_3$. These were performed at the experimental crystal structures[6] using an extended general-potential linearized augmented-plane-wave (LAPW) method,[7–9] which uses a very flexible basis and makes no shape approximations to the potential or charge density and is therefore well suited to materials like the skutterudites with complex structures, low-site symmetries, and transition-metal atoms. Both core and valence electrons were treated self-consistently, the core electrons relativistically in an atomiclike approximation and the valence electrons in a scalar relativistic approximation. Spin-orbit interactions were included in a second variational step for $IrSb_3$ but were found to have only minor effects on the band dispersions. Spin-orbit effects were neglected in the calculations for $CoSb_3$ and $CoAs_3$ where they are presumably smaller. The Hedin-Lundqvist[10] exchange-correlation functional was used with highly converged basis sets chosen for sub-mRy level convergence.[11]

The calculated band structures of $IrSb_3$, $CoAs_3$, and $CoSb_3$ are shown in Figs. 1–3, respectively. The corresponding total and projected electronic densities of states (DOS) are shown in Fig. 4 for $IrSb_3$; the DOS of the Co-based materials are qualitatively similar. In all three materials there is a well-defined gap between the valence and conduction bands, and this is clearly reflected in the DOS in accord with expectations of a band gap. Both the valence and conduction bands are derived from hybridized combinations of transition-metal d and pnictide p states; the p-derived component of the density of states is remarkably flat and symmetrical about the gap, while the d-derived component is peaked below the gap, most strongly for the Co compounds as may be expected from the more spatially localized Co $3d$ orbital relative to the Ir $5d$ orbital. Neglecting the gap-crossing band (discussed below), all three materials have an indirect gap from P to Γ. The local-density approximation (LDA) values of these indirect pseudogaps are 0.71, 0.57, and 0.73 eV for $IrSb_3$, $CoSb_3$, and $CoAs_3$, respectively; the corresponding direct gaps at Γ are 1.21, 0.80, and 0.95 eV. The direct value of 1.21 eV for $IrSb_3$ corresponds reasonably for LDA calculations, with the optical gap of 1.4 eV deter-

0163-1829/94/50(15)/11235(4)/$06.00

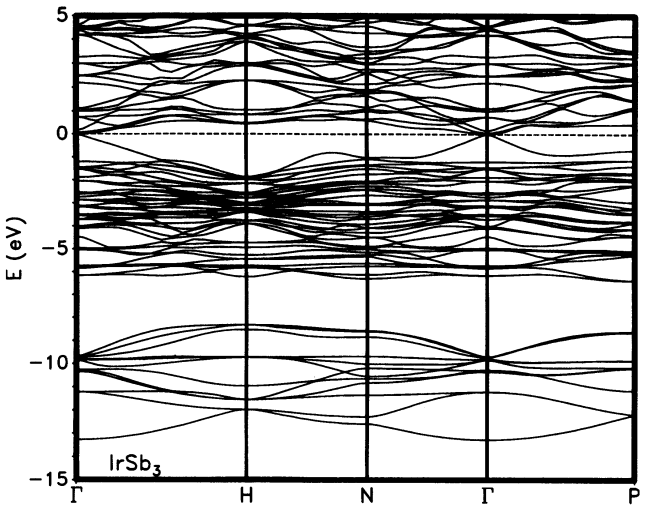

FIG. 1. Band structure of skutterudite $IrSb_3$. The dashed horizontal line denotes the undoped Fermi energy. Spin-orbit effects were included in a second variational step.

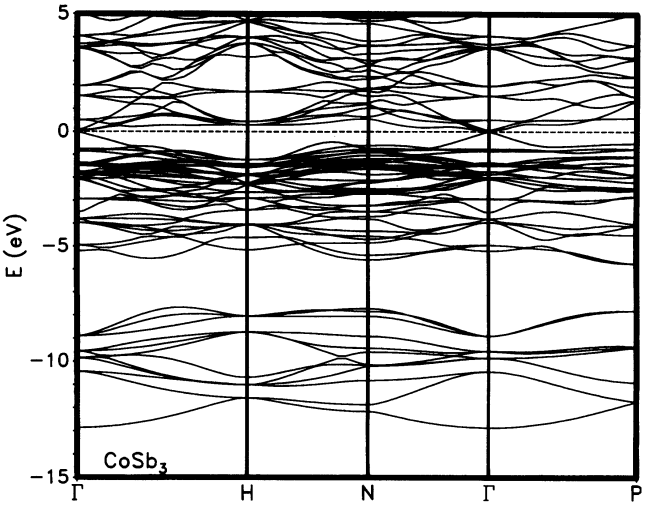

FIG. 3. Scalar relativistic band structure of $CoSb_3$ in the skutterudite structure.

mined by ST (Ref. 2), while the indirect gap of 0.57 eV for $CoSb_3$ is in good agreement with an estimate of 0.5 eV made at high temperature.[12]

However, in addition to the valence and conduction bands discussed above there is a single band that crosses the gap, touching (or very nearly so in $CoSb_3$) the conduction-band minimum at the Γ point. This band is also of hybridized transition-metal d and pnictide p character, though away from the Γ point it has considerably more pnictide p character than the conduction-band minimum, which is dominated by transition-metal d-like contributions. Thus, contrary to expectations, $IrSb_3$ and $CoAs_3$ are predicted to be zero-gap semiconductors; $CoSb_3$ has a very narrow direct gap of 50 meV. This is not due to the lifting of any accidental degeneracy (there is none), but rather to a reordering of the bands. The lowest scalar relativistic bands at and above the Fermi energy at Γ in these materials are (1) a singly degenerate band of p-like character (and no transition-metal s or d character), (2) a twofold-degenerate hybridized band, which differs from the threefold band, below, in having zero metal s character, and being more strongly pnictide p-like although still retaining a dominant metal d component, and (3) a threefold-degenerate hybridized band. In $CoAs_3$ the ordering is (3), (2), (1), while in $CoSb_3$ the ordering is (1), (3), (2). In

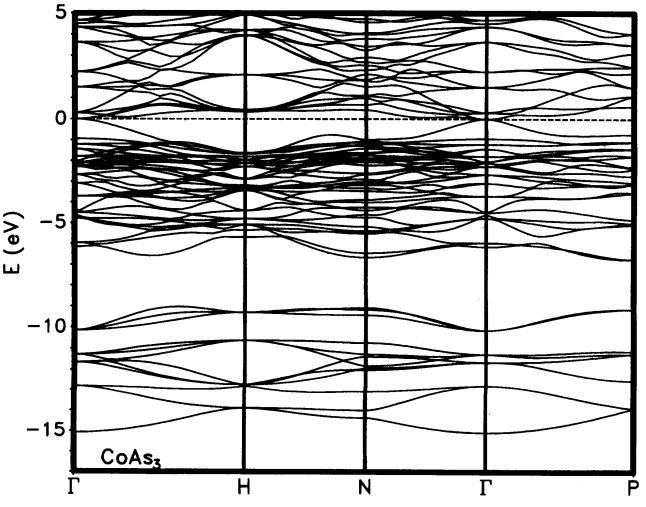

FIG. 2. Scalar relativistic band structure of $CoAs_3$ in the skutterudite structure.

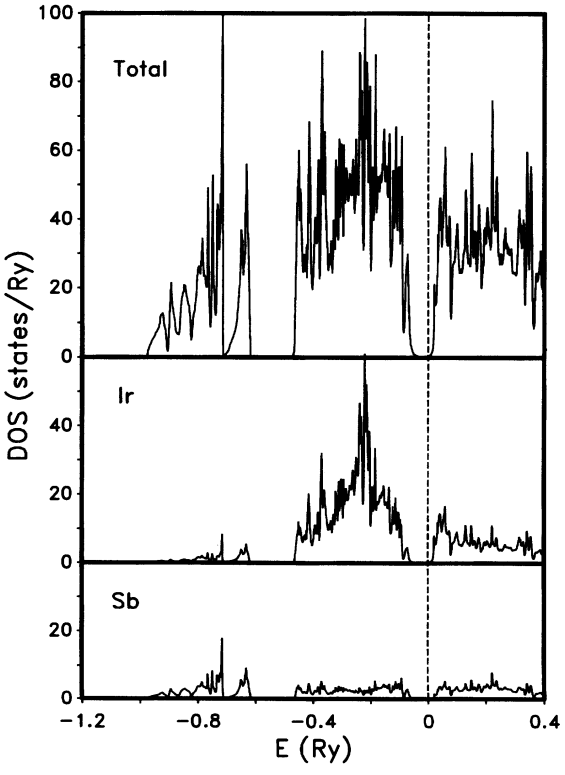

FIG. 4. Electronic DOS and projections onto LAPW spheres for $IrSb_3$. The projections are on a per atom basis, while the total DOS is per formula unit.

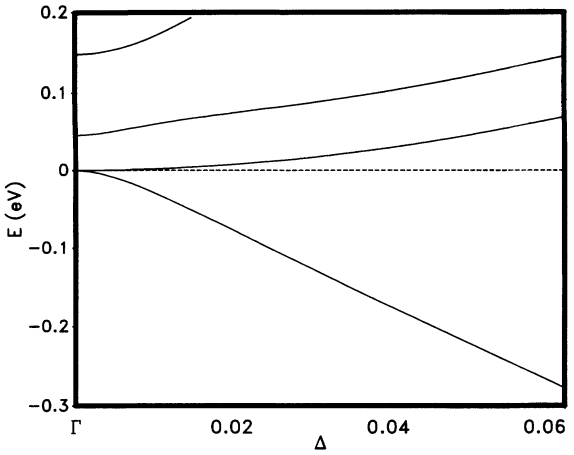

FIG. 5. Blowup of the band structure of Fig. 1 near the Fermi energy along the Γ-H line. The H point corresponds to $\Delta=0.5$. Note the energy scale.

scalar relativistic calculations for $IrSb_3$ the ordering is also different, i.e., (3), (1), (2); the spin-orbit interaction splits (3) into two components with the twofold-degenerate component having the lowest energy, thus retaining the zero gap. Parallel calculations were performed for $IrSb_3$ for a modified crystal structure with 0.05-Å Sb displacements.[13] In this case, the ordering is again changed [to (1), (3), (2) with a 0.1-eV gap], although the linear dispersion of the gap-crossing band is unaffected.

Because of the strong dispersion of the gap-crossing state and because it is just a single band in a unit cell containing many atoms, it provides a relatively small DOS in the gap region that may be difficult to detect. On the other hand, transport measurements and their temperature dependence for hole-doped samples should reflect the properties and existence of this gap-crossing band.

The dispersion of the gap-crossing band is remarkable. Although it has a normal parabolic shape in $CoAs_3$, in $IrSb_3$ and $CoSb_3$ the dispersion, although parabolic in a very small region ($\sim 10^{-5}$ of the zone) near the Γ point, rapidly becomes linear in energy at small wave vectors. A blowup of the band structure for $IrSb_3$ near the Γ point along the Γ-H line is shown in Fig. 5. The crossover between parabolic and linear dispersion occurs for wave vectors between 1% and 2% of the distance to the zone boundary in both $IrSb_3$ and $CoSb_3$, corresponding to hole-doping levels of approximately 3×10^{16} cm^{-3} in both materials. The slopes of the linear dispersing bands are $\alpha=-3.45$ eV Å for $IrSb_3$ and $\alpha=-3.10$ eV Å for $CoSb_3$. Since the reported hole-doping levels in these materials are considerably higher than this, their transport properties are expected to be strongly modified from standard semiconductor behavior by the linear dispersion. Besides the different energy dependence of the DOS (quadratic vs square root) and number of carriers (cubic vs $\frac{3}{2}$ power), the effective inverse mass tensor $\nabla_i\nabla_j\varepsilon(\mathbf{k})$ normally diagonal near a band edge, is entirely off-diagonal corresponding to an "infinite" transport mass normal to the Fermi surface and a doping-level-dependent cyclotron mass given by k/α, where k is the magnitude of the Fermi wave vector (proportional to $n^{1/3}$). Where the constant scattering-time τ approximation holds, the hole mobility μ_h, normally independent of doping level n, varies as $n^{-1/3}$. These predictions may be tested by measuring the cyclotron mass and μ_h for a series of hole-doped samples with different doping levels. The predicted changes of roughly a factor of 2 for a tenfold change in the doping level should be detectable. The Hall number yields the number of carriers in exactly the same way as for a parabolic band provided that the dispersion and scattering are isotropic, which should hold in these lightly doped cubic skutterudites. The degenerate Seebeck coefficient within the constant τ approximation is given by

$$S=-(2\pi k_B^2 T/3e\alpha)(\pi/3n)^{1/3}. \quad (1)$$

This expression has a different doping dependence than with a normal parabolic band. However, as in the parabolic case, τ does not enter the expression for the Seebeck coefficient within the constant τ regime. Because of this, S can be unambiguously calculated, given the temperature and doping level (which may be determined from the Hall number without assumptions regarding the dispersion). Using the value of 1.1×10^{19} holes/cm^3 measured by ST (Ref. 2) for $IrSb_3$ and our calculated value of α, we obtain $S=62$ μV/K at 300 K and $S=123$ μV/K at 600 K. The very close agreement with the experimentally determined Seebeck coefficients of 72 and 126 μV/K measured at 300 and 600 K, respectively, strongly supports our band-structure model. Regarding optimization of the materials for TE applications, the present results predict weaker doping-level dependencies of S and σ as well as the numerator of Z, σS^2, than in ordinary semiconductors. This suggests an emphasis on reducing κ as opposed to optimizing the doping.

Any band with zero slope at Γ and the zone boundary must have a vanishing curvature and therefore linear dispersion somewhere in the zone. The proximity of the linear-dispersing region to the band edge makes the skutterudite antimonides unique. It will be of considerable interest to determine the precise origin of the linear dispersion so near Γ. The electrical properties of $CoSb_3$ and $IrSb_3$ are predicted to be determined by the linear dispersion for moderate levels of hole doping as low as 3×10^{16} cm^{-3}. Above this doping level the properties are predicted to deviate from normal behavior, providing a rare window into the transport properties of semiconductors.

We are grateful for helpful discussions with H. B. Lyon, Jr., G. A. Slack, J. P. Fleurial, and D. Morelli. We thank the authors of Ref. 1 for a prepublication copy of their manuscript. This work was supported by the Office of Naval Research. Computations were performed at the Cornell National Supercomputer Facility and at the DOD computing center at CEWES.

[1] T. Caillat, A. Borshchevsky, and J. P. Fleurial, in *Proceedings of the Eleventh International Conference on Thermoelectrics, Arlington, Texas*, edited by K. R. Rao (University of Texas at Arlington Press, Arlington, 1993).

[2] G. A. Slack and V. G. Tsoukala, J. Appl. Phys. **76**, 1665 (1994).

[3] G. A. Slack, in *Solid State Physics*, edited by H. Ehrenreich, F. Seitz, and D. Turnbull (Academic, New York, 1979), Vol. 34, p. 1.

[4] Note that there are three anions for each cation and that with the exception of $CoSb_3$, where the mass ratio is 0.79, the anion is by far the lighter component. Thus the thermal conductivities may not be strongly affected by these substitutions on the cation site, whereas substituting lighter anions (e.g., As) may give higher and less favorable values of κ.

[5] J. Ackermann and A. Wold, J. Phys. Chem. Solids **38**, 1013 (1977).

[6] P. Villars and L. D. Calvert, *Pearson's Handbook of Crystallographic Data for Intermetallic Phases*, 2nd ed. (American Society for Metals, Metals Park, OH, 1991).

[7] D. Singh, Phys. Rev. B **43**, 6388 (1991).

[8] O. K. Andersen, Phys. Rev. B **12**, 3060 (1975).

[9] S. H. Wei and H. Krakauer, Phys. Rev. Lett. **55**, 1200 (1985); D. J. Singh, *Planewaves, Pseudopotentials and the LAPW Method* (Kluwer Academic, Boston, 1994), and references therein.

[10] L. Hedin and B. I. Lundqvist, J. Phys. C **4**, 2064 (1971).

[11] LAPW sphere radii of 2.2 a.u. were used for all elements except Ir, for which a radius of 2.35 a.u. was used. Basis sets consisting of approximately 3000 functions were used for $IrSb_3$ and $CoSb_3$, while approximately 2200 functions were used for $CoAs_3$, which has a considerably smaller cell volume than the antimonides. Local orbitals were used to relax any errors due to linearization of the Ir $5d$ bands and to include the Sb $4d$ states in the valence window. The zone sampling was carried out with eight special points in the irreducible wedge of the bcc zone. Note that the unit cell contains 16 atoms.

[12] L. D. Dudkin and N. K. Abrikosov, Zh. Neorg. Khim. **1**, 2096 (1956) [Russian J. Inorg. Chem. **1**, 169 (1956)].

[13] A. Kjekshus and T. Rakke, Acta Chemica Scand. A **28**, 99 (1974).